JCI insight

RESEARCH ARTICLE

HSV-2 ΔgD elicits FcγR-effector antibodies that protect against clinical isolates

Christopher D. Petro,[1,2,3] Brian Weinrick,[1,2] Nazanin Khajoueinejad,[3] Clare Burn,[1,3] Rani Sellers,[4] William R. Jacobs Jr,[1,2] and Betsy C. Herold[1,3]

[1]Department of Microbiology and Immunology, [2]Howard Hughes Medical Institute, [3]Department of Pediatrics, [4]Histology and Comparative Pathology Facility, Albert Einstein College of Medicine, Bronx, New York, USA.

A single-cycle herpes simplex virus (HSV) deleted in glycoprotein D (ΔgD-2) elicited high titer HSV-specific antibodies (Abs) that (i) were rapidly transported into the vaginal mucosa; (ii) elicited antibody-dependent cell-mediated cytotoxicity but little neutralization; (iii) provided complete protection against lethal intravaginal challenge; and (iv) prevented establishment of latency in mice. However, clinical isolates may differ antigenically and impact vaccine efficacy. To determine the breadth and further define mechanisms of protection of this vaccine candidate, we tested ΔgD-2 against a panel of clinical isolates in a murine skin challenge model. The isolates were genetically diverse, as evidenced by genomic sequencing and in vivo virulence. Prime and boost immunization (s.c.) with live but not heat- or UV-inactivated ΔgD-2 completely protected mice from challenge with the most virulent HSV-1 and HSV-2 isolates. Furthermore, mice were completely protected against 100 times the lethal dose that typically kills 90% of animals (LD90) of a South African isolate (SD90), and no latent virus was detected in dorsal root ganglia. Immunization was associated with rapid recruitment of HSV-specific FcγRIII- and FcγRIV-activating IgG2 Abs into the skin, resolution of local cytokine and cellular inflammatory responses, and viral clearance by day 5 after challenge. Rapid clearance and the absence of latent virus suggest that ΔgD-2 elicits sterilizing immunity.

Introduction

Herpes simplex virus serotypes 1 and 2 (HSV-1 and HSV-2) are significant global health problems that disproportionately impact developing countries and further fuel the HIV epidemic. HSV-2 is the leading cause of genital ulcerative disease worldwide, whereas HSV-1 has emerged as the more common cause of genital infection in industrialized nations (1). Perinatal transmission of either serotype can result in severe infant morbidity or death. Moreover, HSV-1 is the most common cause of sporadic fatal encephalitis in the US, and even with optimal i.v. acyclovir therapy, mortality is 14%–19% and fewer than 50% of survivors are able to resume a normal lifestyle (2). A more recent epidemiological study estimates HSV-2 prevalence at 517 million globally with 21 million new infections annually; this is marked by exceedingly high prevalence rates (~90%) in sub-Saharan Africa (3–5). Importantly in areas with high HSV-2 prevalence, infection with HSV-2 promotes HIV acquisition, and coinfection is associated with increased rates of HIV and HSV shedding as well as increased frequency and/or severe episodes of HSV reactivation (6–8). These findings underscore the need to develop an effective vaccine against both HSV serotypes.

The primary focus of HSV vaccine development has been the induction of high levels of neutralizing antibody responses targeting glycoprotein D (gD) with either subunit adjuvant vaccines or attenuated strains. Despite the preclinical findings of a reduction in primary and recurrent disease in murine or guinea pig models, the most recent gD subunit vaccine (HerpeVac) failed to protect against HSV-2 in clinical trials. Moreover, post hoc analysis found that gD neutralizing antibody titers in serum did not correlate with HSV-2 protection, highlighting the need for alternative vaccine approaches and surrogates of immunity (9). No other candidate correlates of protection, such as mucosal antibody levels, subclass distribution, or nonneutralizing antibody effector functions, were measured in the preclinical or clinical trials.

A second potential limitation of prior preclinical vaccine work is that most of the animal studies were conducted using 1 or 2 laboratory strains such as HSV-2(MS) and HSV-1(17) or HSV-1(McKrae)

Conflict of interest: The authors CDP, WRJJ, and BCH are inventors on a pending patent on the HSV-2 ΔgD-2 vaccine.

Submitted: May 10, 2016
Accepted: June 30, 2016
Published: August 4, 2016

Reference information:
JCI Insight. 2016;1(12):e88529.
doi:10.1172/jci.insight.88529.

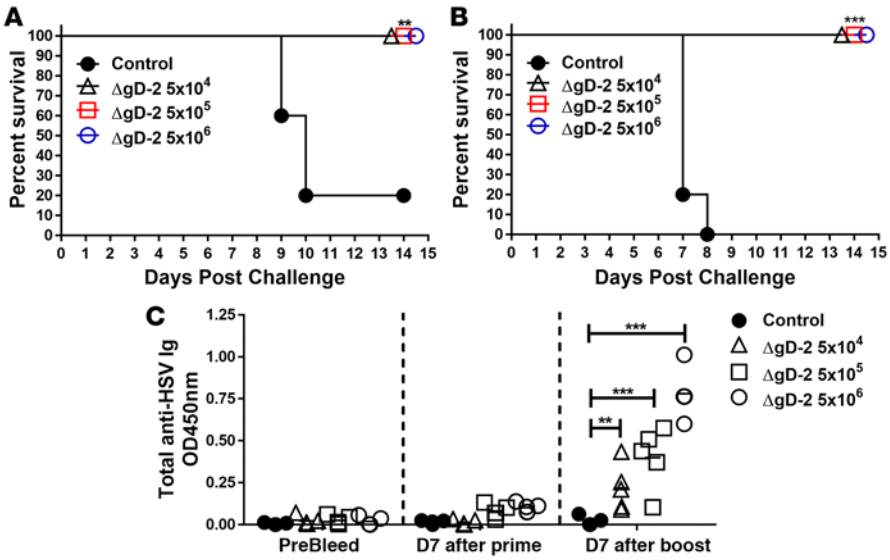

Figure 1. HSV-2ΔgD-2 provides complete protection following intravaginal or skin challenge with vaccine doses as low as 5×10^4 PFU. C57BL/6 mice were primed and, 21 days later, were boosted s.c. with 5×10^4 PFU, 5×10^5 PFU, or 5×10^6 PFU of HSV-2 ΔgD-2 or VD60 lysates (control). Mice were subsequently challenged 21 days after boost with an LD90 of HSV-2(4674) either (**A**) intravaginally or (**B**) via skin scarification and followed for survival (n = 5 mice/group). (**C**) Serum was assessed for HSV-2 antibodies by ELISA before (PreBleed), day 7 after prime, and day 7 after boost; each symbol represents optical densitometry units (OD) for an individual mouse (n = 5/group); lines represent mean of each group. ΔgD-2– and control-vaccinated groups were compared for survival by Kaplan-Meier and for Ab responses by 2-way ANOVA; $^{**}P < 0.01$, $^{***}P < 0.001$.

(10–12). Importantly, recent whole-genome sequencing of multiple HSV-1 and HSV-2 isolates indicates that, despite featuring highly conserved genomes (<4% and <0.5% intranucleotide diversity, respectively), there is substantial divergence at the amino acid level (13–15). Divergence between clinical isolates appears to be linked to differences between tegument and glycoprotein including VP22, gG, gE, and gI (13, 16). This diversity may be reflected in antigenic variation (as observed between the 2 serotypes for gG) and could reduce the efficacy of vaccines (17), especially if the vaccines rely on a limited number of viral antigens to elicit protection.

We previously reported a single-cycle vaccine approach in which we engineered an HSV-2(G) virus deleted in U_s6 (*gD*) and complemented the virus by growing it on a Vero cell line that expresses HSV-1 gD (VD60 cells) (18). Immunization with the complemented virus (designated ΔgD-2) provided complete protection against lethal vaginal and skin challenge with a single isolate of HSV, HSV-2(4674), and no virus was detected in dorsal ganglia (DRG) by PCR or ex vivo coculture, indicating that the vaccine protected against the establishment of latency defined herein as sterilizing immunity. The vaccine elicited high-titer HSV-specific Abs that had little neutralization activity (neutralization titer 1:5) but elicited antibody-dependent cell-mediated cytotoxicity (ADCC). Protection was transferred to naive mice by a single dose of immune serum but was lost when transferred into Fc receptor (FcR) KO or Fc neonatal receptor KO mice (19).

Building on this background, the current studies were designed to test the ability of this vaccine candidate to protect against clinical HSV-1 and HSV-2 isolates and to further define the mechanism of protection focusing on local immune response at the site of infection. The most commonly used model of HSV-2 is the murine intravaginal challenge model, which requires pretreatment of mice with progesterone for consistent infection. However, since most clinical disease occurs on the skin following breaches in the epithelial barrier (20), we focused primarily on a skin scarification model, which displays viral kinetics and histopathology similar to humans and does not require progesterone pretreatment (21).

Results

Immunization with low doses of ΔgD-2 is protective against lethal skin and intravaginal challenge. C57BL/6 mice (5 mice per group) were s.c. primed and then boosted 21 days later with 5×10^4, 5×10^5, or 5×10^6 PFU of ΔgD-2. Three weeks later, the mice were challenged either intravaginally (following pretreatment with medroxyprogesterone) or by skin scarification with a lethal dose that typically kills 90% of animals (LD90) (5×10^5 PFU) of HSV-2(4674), a previously described clinical isolate (22). All HSV-2 ΔgD-2 immunized mice survived (5/5 per group), whereas all of the control-vaccinated mice (immunized with VD60 cell lysate) succumbed to disease (Figure 1, A and B). Although the mice vaccinated with the lowest dose (5×10^4) showed mild epithelial disease (Supplemental Figure 1, A and B; supplemental material available online with this article; doi:10.1172/jci.insight.88529DS1), no signs of neurological disease were observed and all animals completely recovered by day 14 in both challenge models. HSV-specific Abs (measured by

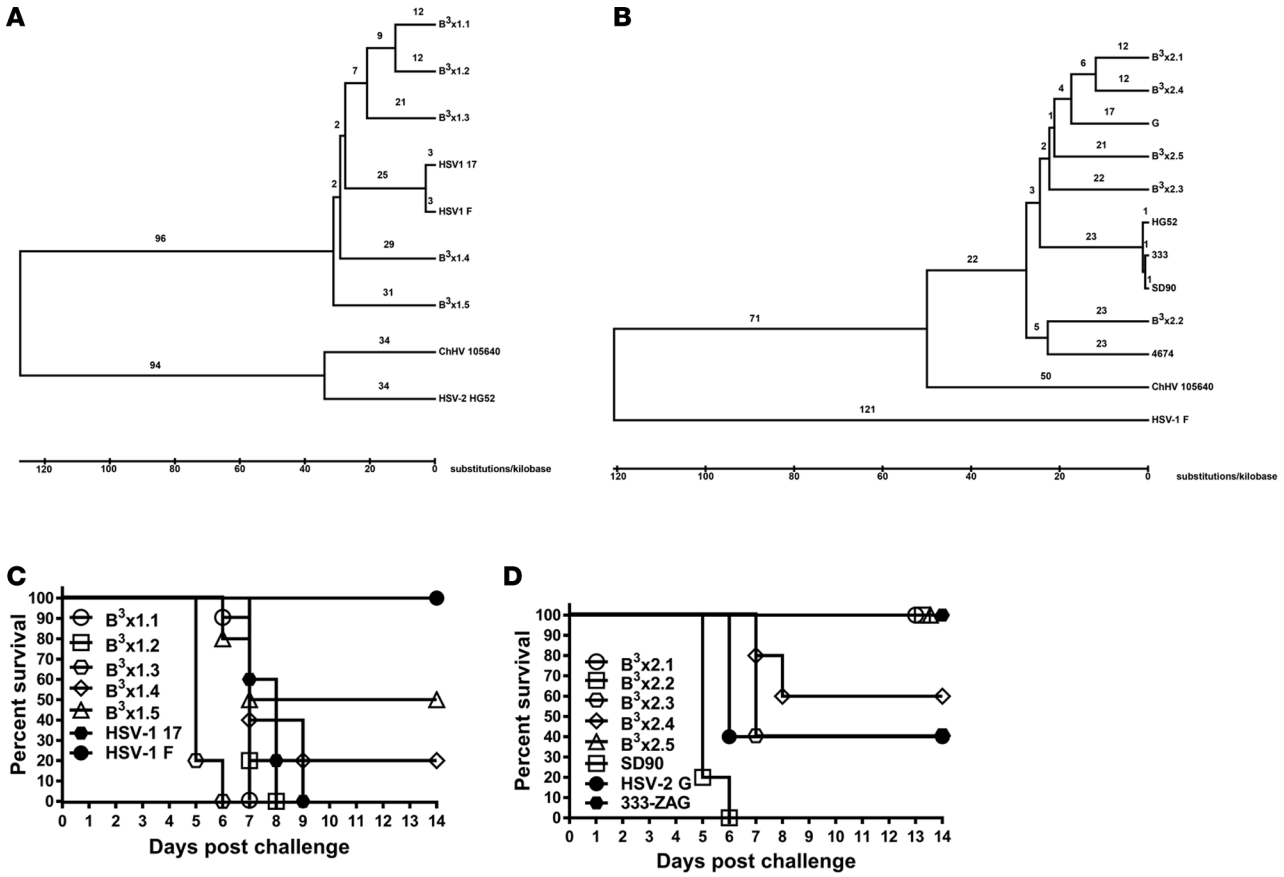

Figure 2. Clinical HSV-1 and HSV-2 isolates are genotypically and phenotypically diverse. (**A**) Herpes simplex virus type-1 (HSV-1) and (**B**) HSV-2 phylogenic trees were constructed from whole genome alignments of de novo–assembled HSV clinical isolate and lab strain sequences by the UPGMA method in MEGA6. The branches are labeled with genetic distance in nucleotide substitutions/kilobase. All branches in HSV-1 tree showed 100% confidence; those on the HSV-2 tree were also 100% except the branches at the level of 4674, which were 92%, and the branch bearing $B^3 \times 2.3$, which was 99%. Published data for Chimpanzee α-1 herpesvirus (ChHV), HSV-1(F), or HSV-2(HG52) were used as outgroups for each analysis. (**C**) In vivo virulence was assessed by challenging BALB/C mice with 1×10^5 PFU/mouse of HSV-1 (**D**) or 5×10^4 PFU/mouse of HSV-2 by skin scarification. Survival curves are shown for each isolate; open symbols represent clinical isolates, and closed symbols represent laboratory strains.

ELISA using infected cell lysate as the antigen) were detected in the serum of all vaccinated mice one week after boost, but not prime, and the Ab titer increased with administration of higher vaccine doses (Figure 1C).

Mice immunized with ΔgD-2 are protected from high viral challenges of virulent HSV-1 and HSV-2 clinical isolates. To evaluate if the ΔgD-2 vaccine protects against diverse HSV-1 and HSV-2 strains, we obtained 5 HSV-1 (denoted $B^3 \times 1.1$ – $B^3 \times 1.5$) and 5 HSV-2 (denoted $B^3 \times 2.1$ – $B^3 \times 2.5$) clinical isolates from the Clinical Virology Lab at Montefiore (Bronx, New York, USA), as well as a previously described South African HSV-2 clinical isolate (SD90, ref. 17). The isolates were grown on Vero cells and were passaged no more than 3 times before sequencing and phenotyping. Illumina sequencing (Figure 2, A and B) showed that the strains exhibited substantial genetic diversity with pairwise distances as high as 6.3% between $B^3 \times 1.5$ and the other $B^3 \times 1$ isolates and 5.0% between $B^3 \times 2.2$ and the other $B^3 \times 2$ isolates. In vivo virulence of each clinical strain was compared with laboratory strains by challenging BALB/C mice using the skin scarification model with 1×10^5 PFU of the HSV-1 strains or 5×10^4 PFU of HSV-2 strains (Figure 2, C and D). The clinical isolates demonstrated a range of virulence with $B^3 \times 1.1$, $B^3 \times 1.3$, $B^3 \times 2.3$, and SD90 inducing more rapid disease, with the highest morbidity (Figure 2, C and D; Supplemental Figure 2, A and B). Similar results were observed in the vaginal challenge model, with the same 4 isolates exhibiting the most virulent disease (not shown). Interestingly, no significant differences between the isolates were observed by in vitro single and multistep growth curves on Vero cells (Supplemental Figure 3, A and B).

To assess whether ΔgD-2 protected against the different isolates, C57BL/6 or BALB/C mice were

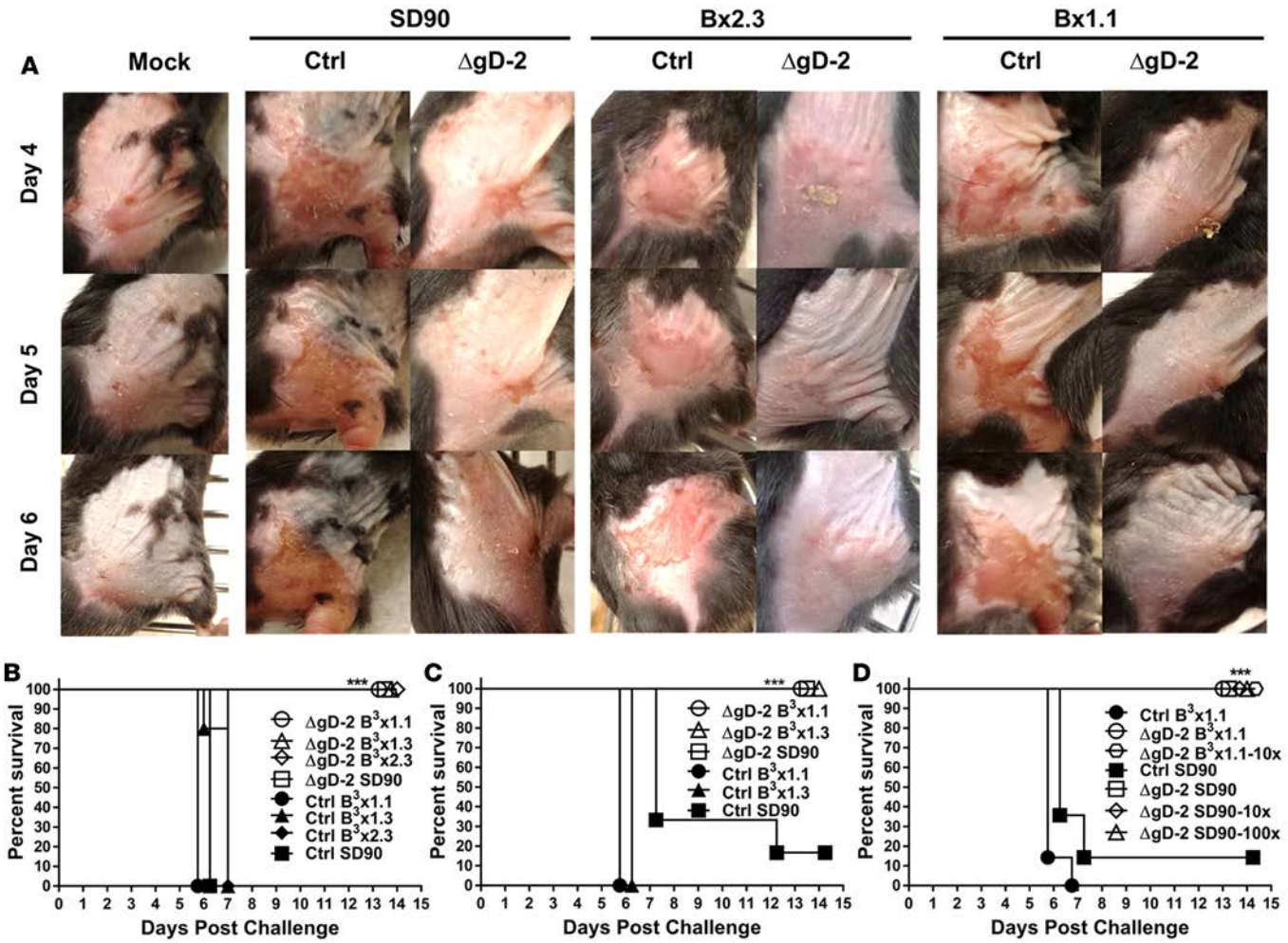

Figure 3. HSV-2 ΔgD-2 protects mice from clinical isolates of HSV-1 and HSV-2. C57BL/6 (n = 7 mice/group) or BALB/C (n = 5 mice/group) mice were immunized with ΔgD-2 or VD60 cell lysates (control) and subsequently challenged by skin scarification with an LD90 dose of the most virulent isolates and monitored daily. (**A**) Representative images from C57BL/6 mice on days 4, 5, and 6 after challenge (magnification 1.2×); (**B**) survival curves for C57BL/6 mice, and (**C**) survival curves for BALB/C mice. (**D**) Additional C57BL/6 mice were challenged with 10 and 100 times (10x and 100x) the LD90 dose of SD90 and 10 times the LD90 of B^3 × 1.1. ΔgD-2 and control-vaccinated groups were compared for survival by Kaplan-Meier; ***P < 0.001.

primed and boosted with 5 × 10^6 PFU/mouse of ΔgD-2 (or VD60 lysate as the control immunogen) and then challenged with an LD90 dose of the 4 more virulent clinical isolates (Table 1) using the skin scarification model. All ΔgD-2–vaccinated mice survived challenge (n = 7 C57BL/6 mice per group, Figure 3, A and B; n = 5 BALB/C mice per group, Figure 3C). While some mice exhibited mild epithelial disease, which peaked on day 4, the majority of animals had fully recovered by day 8 after challenge (Supplemental Figure 4, A and B). No signs of neurological disease were detected in any of the mice at any time point.

To further evaluate the robustness of the immune response, we increased the challenge dose in the C57BL/6 mice to 10 times and 100 times the LD90 doses of SD90 and 10 times the LD90 of B^3 × 1.1. All of the ΔgD-2–vaccinated mice survived (Figure 3D) with no signs of neurological disease (Supplemental Figure 4C). The ΔgD-2–vaccinated mice had significantly less infectious virus detected in skin biopsies by plaque assay on day 5 after challenge (Figure 4A, n = 3 mice per group). Histopathology of skin biopsies revealed ulceration and necrosis covering 75%–95% of the epithelium in control-vaccinated mice compared with < 10% epithelial necrosis and ulceration in the ΔgD-2–vaccinated mice; the histopathological findings in ΔgD-2–vaccinated mice resembled those of the unvaccinated, uninfected controls that were treated with depilation and skin scarification (Supplemental Figure 5). Moreover, there was no replicating or latent virus detected by plaque assay (Figure 4B) or quantitative PCR (qPCR) (Figure 4C), respectively, in DRGs isolated on day 14 after challenge in the ΔgD-2–vaccinated mice (n = 5 mice per each challenge dose and

Table 1. HSV strains used in vaccine efficacy studies

Viral Strain	Origin of Isolate	HSV Serotype	Lethal Dose$_{90}$[A]
B^3 × 1.1	United States	Type 1	5 × 10^5 PFU
B^3 × 1.3	United States	Type 1	1 × 10^5 PFU
SD90	South Africa	Type 2	5 × 10^4 PFU
B^3 × 2.3	United States	Type 2	1 × 10^5 PFU
4674	United States	Type 2	5 × 10^5 PFU

[A]PFUs that cause 90% morbidity in BALB/C mice skin challenge model

strain). Similarly, we did not detect any reactivating virus when DRGs from ΔgD-2–vaccinated mice (isolated day 5 after challenge with LD90 of SD90) were cocultured for 3 weeks with Vero cells. In contrast, viral DNA and reactivatable virus were recovered from all control-vaccinated (VD60 cell lysate–vaccinated) mice (DRG isolated at time of euthanasia; Figure 4D, n = 5 mice per group).

To determine if viral gene expression is needed to elicit complete immunity against HSV clinical isolates, we compared the vaccine efficacy of live or inactivated ΔgD-2 stocks. Virus was inactivated by brief exposure to UV light, which allows virus to bind and enter cells but not express viral gene products (Figure 5A) (23) or heat inactivation (HI), which results in virus that does not enter cells. Mice were primed and boosted with 5 × 10^6 PFU of live ΔgD-2, or equivalent particles of UV or HI ΔgD-2 or VD60 lysate, and subsequently challenged with an LD90 dose of HSV-2(SD90) on the skin. HI virus failed to protect against lethal disease with only 1 of 5 mice surviving (Figure 5, B and C) and did not prevent the establishment of latency (Figure 5D). UVΔgD-2–immunized mice survived lethal skin challenge (n = 5 per group, Figure 5B); however, disease scores were higher compared with mice that received live viral vaccine (Figure 5C), and UVΔgD-2 did not prevent establishment of latency (Figure 5D). HSV genomes were detected in the DRG from all of the mice that received HI- or UV-inactivated virus or VD60 control lysates (Figure 5C). In contrast, a low level of HSV DNA was detected in only 1 of 33 mice immunized with live ΔgD-2 (Figures 4, C and D, and Figure 5C).

HSV-2 ΔgD-2 elicits FcγR effector antibodies that are rapidly recruited into the skin following challenge. Serum from ΔgD-2–vaccinated mice obtained 1 week after boost induced antibody-dependent cellular phagocytosis (ADCP) of HSV-coated beads by THP-1 cells with the release of higher levels of IFN-γ compared with serum from VD60 lysate (control) immunized mice, indicative of FcγR effector activity (Figure 6A). Consistent with this, ΔgD-2 serum obtained 1 week after boost and 1 week after challenge activated murine FcγRIV and FcγRIII, whereas control serum showed no mFcγRIV and 23- to 47-fold less mFcγRIII activation at 1 week after challenge (Figure 6B). Furthermore, ΔgD-2 serum was able to activate mFcγRIV when the serum was incubated with cells infected with 5 different clinical isolates (Figure 6C).

To further explore the differences in efficacy observed in response to inactivated ΔgD-2, immune serum obtained 1 week after boost from mice vaccinated with live, UV, or HI ΔgD-2 were assayed for total HSV-specific Abs by ELISA and for mFcγRIV activation. UV or HI ΔgD-2 elicited lower HSV-specific Abs (1:50,000 titer) compared with live viral vaccine (1:250,000; Figure 6D). Moreover, there was a decrease in mFcγRIV activation by immune serum obtained from mice vaccinated with inactivated compared with live ΔgD-2 with HI virus eliciting little FcγR activation (P < 0.01 compared with live ΔgD-2), and UV virus eliciting an intermediate response (Figure 6E). These findings parallel the differences in efficacy (Figure 5).

The presence of HSV-specific Abs was examined 21 days after boost and 2 or 5 days after challenge in skin homogenates by ELISA using either an HSV-2(4674)– or HSV-1(17)–infected cell lysate as the antigen. The ΔgD-2–immunized mice had low levels of HSV-specific Abs in the skin after boost, which rapidly increased as early as day 2 after challenge (Figure 7A). B^3 × 1.1 elicited higher titer Ab response compared with SD90. In contrast, no HSV-specific Abs were detected in the skin of control-vaccinated mice on day 2 or day 5 after challenge (Figure 7, A and B). The Abs recovered from the skin were predominantly IgG (1:24,000 titer; Figure 7B) with no anti–HSV IgA or IgM detected (data not shown), enriched in IgG2 (equal proportions of IgG2a and IgG2b, Figure 7C), and induced mFcγRIV and mFcγRIII activation (data shown for day 2 after challenge, Figure 7D).

HSV-2 ΔgD-2–immunized mice have minimal inflammation following skin HSV challenge. Biopsies were obtained 2 or 5 days after challenge and processed for histology and/or homogenized. They were then evaluated for presence of cytokines/chemokines and neutrophils. Consistent with the histopathology (Supplemental Figure 5), local Ab response (Figure 7), and rapid clearance of virus (Figure 4), there was a decrease in inflammatory cytokines/chemokines detected in skin homogenates in the ΔgD-2–immunized compared with control immunized mice on day 5 after challenge (Figure 8). HSV-1– and HSV-2–infected mice had higher levels of TNFα (Figure 8A), IL-1β (Figure 8B), and IL-6 (Figure 8C) compared with mock-infected

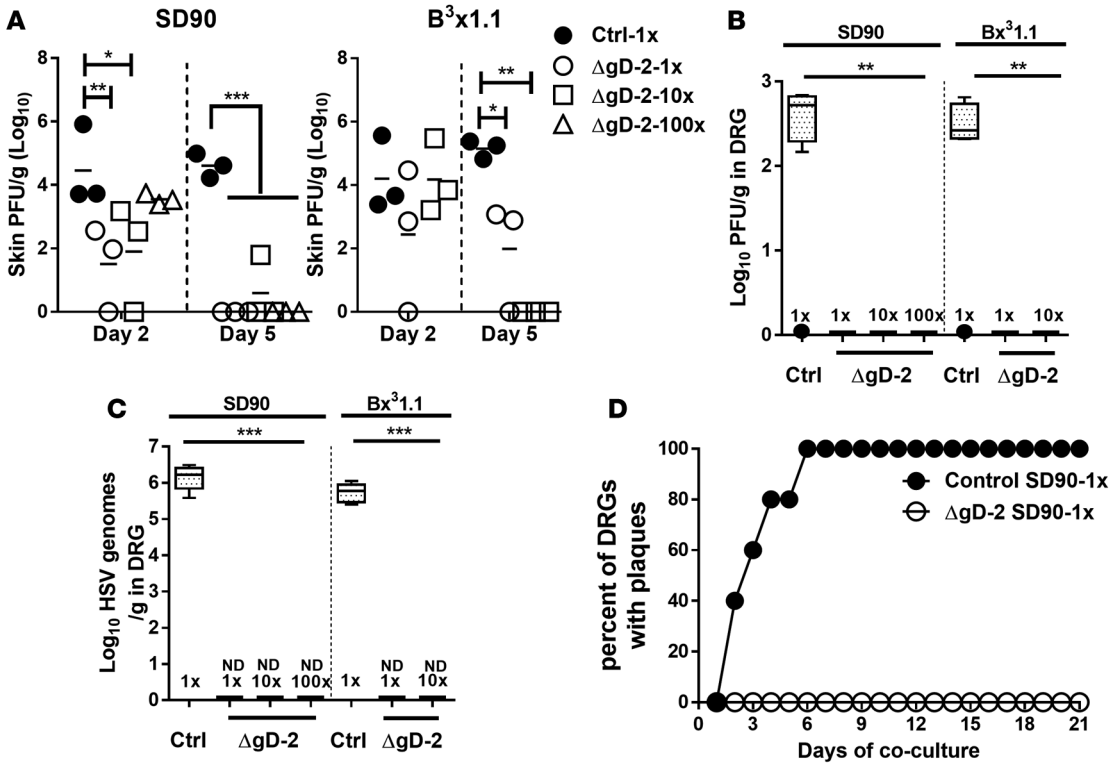

Figure 4. Virus is rapidly cleared and no latent virus is detected in dorsal root ganglia isolated from HSV-2 ΔgD-2–vaccinated mice. Mice were immunized with ΔgD-2 or VD60 cell lysates (control) and subsequently challenged by skin scarification with 1, 10, or 100 times the LD90 of HSV-2(SD90) or with 1 or 10 times the LD90 of HSV-1($B^3 \times 1.1$) (n = 5 mice per group). (**A**) Skin biopsies were obtained on day 2 and day 5 after challenge and assayed for viral load by plaque assay on Vero cells (n = 3 samples/group, lines represent mean). (**B**) Replicating or (**C**) latent HSV in dorsal root ganglia (DRG) tissue obtained from ΔgD-2–vaccinated (day 14 after challenge) or control-vaccinated (time of euthanasia) mice were assessed by plaque assay and qPCR, respectively (n = 5 mice/group). (**D**) Latency was further evaluated by coculturing Vero cells with DRG isolated at day 5 after challenge from ΔgD-2– and control–immunized mice that were challenged with a 1× LD90 of HSV-2 SD90 (n = 5/group). Data in **B** and **C** are presented as box and whisker plots, with the bounds of the box representing the 25th and 75th percentile, the line representing the median, the whiskers representing the 10th and 90th percentile, and black dots indicating outliers. The HSV-2 ΔgD-2–vaccinated group and control–vaccinated groups were compared by student's t test; $^*P < 0.05$; $^{**}P < 0.01$; $^{***}P < 0.001$.

mice on day 2 independent of immunization. However, the levels decreased by day 5 in ΔgD-2 but not the control-immunized mice. Similar results were obtained for the chemokines CXCL9 (Figure 8D) and CXCL10 (Figure 8E). Interestingly, IL-33 levels were consistently higher in ΔgD-2–immunized compared with control-immunized mice at both time points (Figure 8F). A decrease in $Ly6G^+$ neutrophils (Figure 8G) in skin biopsies from ΔgD-2–immunized was observed compared with control-immunized mice.

Discussion

The salient findings from this study are that vaccination with live, single-cycle HSV-2 ΔgD-2 affords complete protection against a panel of genetically diverse HSV-1 and HSV-2 clinical isolates and prevents the establishment of latency using 2 different challenge models (vaginal and skin) and different strains of mice (B6 and BALB/c). We focused predominantly on the skin model — because it may be more reflective of human disease — and provided the opportunity to study the local immune responses. Specifically, we found that ΔgD-2 elicited high-titer IgG Abs that were rapidly recruited into the skin, resulting in clearance of virus by day 5 even following challenge with 100 times the LD90 of the most virulent strain, SD90. The rapidity of viral clearance likely contributed to the vaccine's ability to prevent the establishment of latency, thereby providing sterilizing immunity. The protective effect of ΔgD-2 against a broad array of HSV-1 and HSV-2 clinical isolates differentiates it from other candidate vaccines such as HSV-2 $\Delta U_L5/\Delta U_L29$, which failed to fully protect against the clinical isolate SD90 (17) or gD subunit vaccines that have only been tested against 1 or 2 laboratory strains (10).

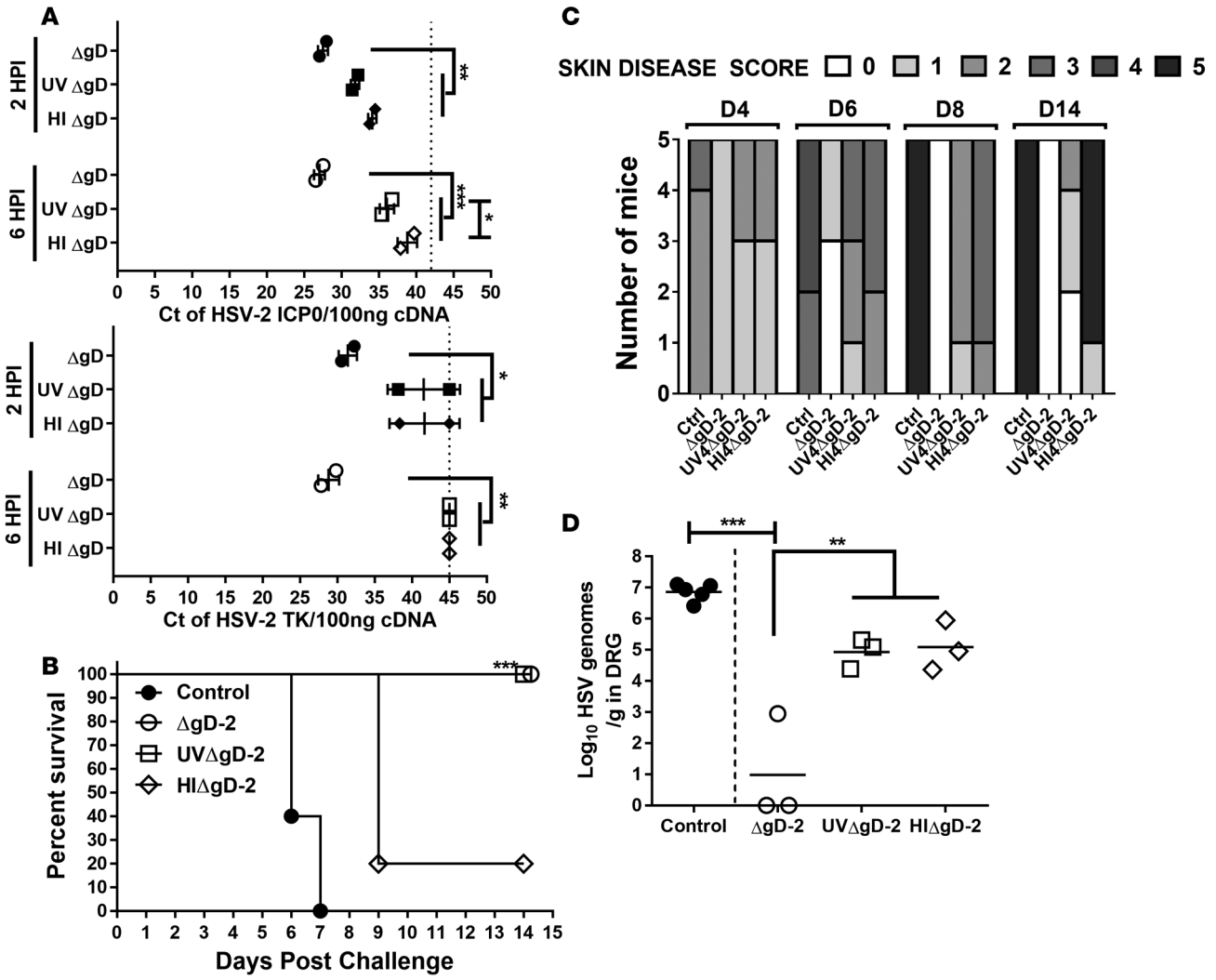

Figure 5. Inactivation of ΔgD-2 leads to reduction in vaccine efficacy. (**A**) Vero cells were infected with an MOI of 5 PFU/cell of ΔgD-2 or an equivalent amount of UV-inactivated (UVΔgD-2) or heat-inactivated (HIΔgD-2) virus and viral gene expression for infected cell protein-0 (ICP0, upper panel) and thymidine kinase (TK, lower panel) assessed at 2 hours (closed symbols) and 6 hours (open symbols) after infection (HPI). Data are presented as threshold cycle (Ct). Each point represents Ct values from individual experiment; lines equals mean ±SD from replicate experiments, with the dotted line indicating the Ct values for mock-infected cells. The asterisks indicate results for 2-way ANOVA comparing UVΔgD-2, HIΔgD-2, and ΔgD-2 Ct values at each time after infection (*$P < 0.05$, **$P < 0.01$, ***$P < 0.001$). (**B** and **C**) Mice were prime-boost vaccinated with 5×10^6 PFU of live or equivalent concentrations of UVΔgD-2, HIΔgD-2, ΔgD-2, or VD60 lysates (control) and subsequently challenged with an LD90 of HSV-2(SD90) on the skin ($n = 5$/group). Mice were monitored for (**B**) survival and (**C**) skin disease scores. Kaplan Meier analysis was used for survival curves of ΔgD-2–, UVΔgD-2–, HIΔgD-2–, and control-vaccinated mice. (**D**) At day 5 after challenge, mice were euthanized and DRGs were extracted for qPCR analysis of HSV DNA ($n = 3$/group for UV-, HI-, or ΔgD-2–immunized mice or $n = 5$ for control-treated mice; lines represent the mean). **$P < 0.01$, ***$P < 0.001$ by 2-way ANOVA, ΔgD-2–vaccinated groups vs. control-vaccinated group.

The broad protection afforded by ΔgD-2 likely reflects the unique nature of the immune response elicited. Consistent with our initial studies (19), we found that the Abs induced were enriched for the IgG2 subtype (~80% of all HSV-specific IgG in the skin), reached high titers (1:24,000) in skin biopsies by day 2 after challenge, and had low-level neutralizing activity (19) but mediated several Fc effector functions, including ADCP (shown here) and ADCC (19). The ability to activate the murine FcγRIV, which is strongly associated with ADCC (24), was confirmed using a quantitative reporter assay with target cells infected by different clinical isolates. The antibody response to ΔgD-2 was viral gene expression–dependent, as evidenced by disease scores, total Ab titers, and antibody-mediated mFcγRIV activation in dose escalation and viral inactivation experiments. Murine FcγRIV activation correlated with protection, as evidenced by the parallel decrease in both response to UV and HI virus. The specific antigenic targets of the FcγR-activating Abs are currently being investigated, but the decreased response to UV-inactivated compared with

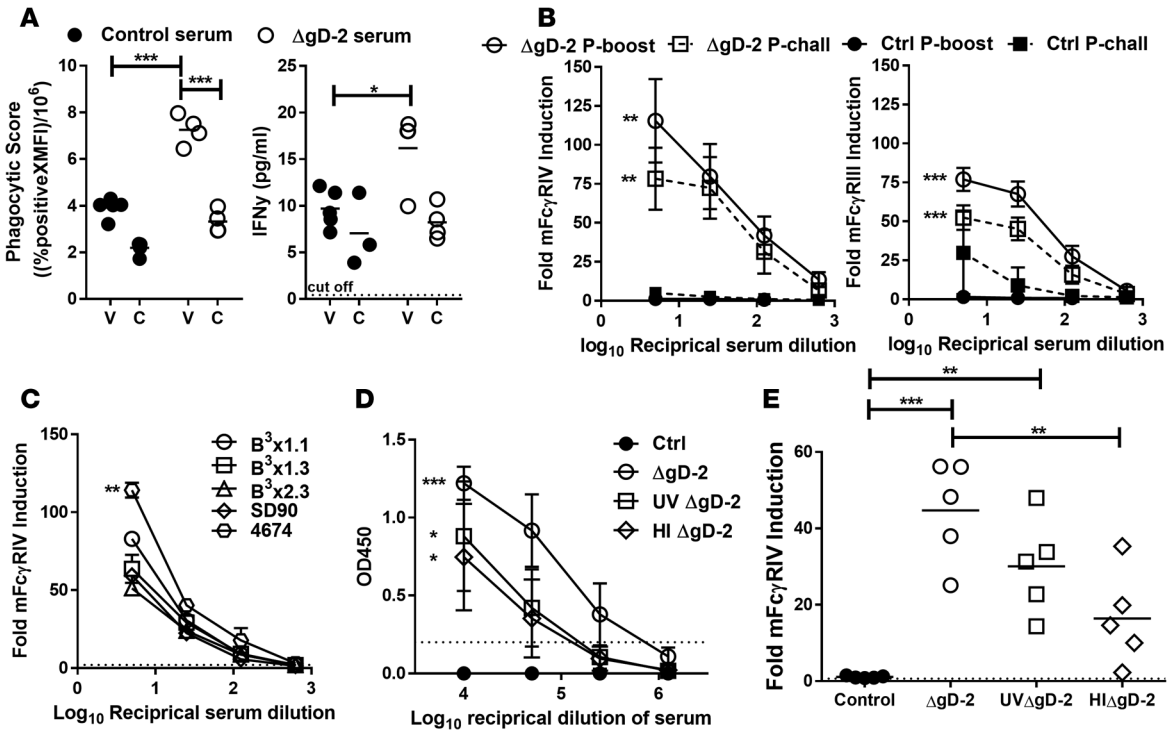

Figure 6. HSV-2 ΔgD-2 elicits cross-reactive HSV-specific FcγR effector antibodies. Mice were vaccinated with ΔgD-2 or VD60 lysates (control) and subsequently challenged with HSV-2(4674) on the skin (n = 5/group). (**A**) Antibody-dependent cellular phagocytosis (ADCP) activity of serum from control or HSV-2 ΔgD-2–vaccinated mice 7 days after boost was quantified using THP-1 monocytic cell line and beads coated with HSV-2–infected cell lysates (v) or uninfected cell lysates (c) (left panel). The %ADCP is calculated as percent of cells positive for beads multiplied by the MFI of positive cells divided by 1×10^6. IFN-γ levels were measured in the supernatants 8 hours after incubation of THP-1 cells with the beads (right panel) (n = 4/group, line represents the mean). (**B**) Serum from 7 days postboost or 7 days postchallenge ΔgD-2– or control-immunized mice were further assessed for mFcγRIV (left panel) and mFcγRIII (right panel) activation via a luciferase effector cell reporter assay using HSV-2(4674)–infected target cells (data represented as mean ±SD values of 5 mice/group). (**C**) ΔgD-2 boost serum was pooled day 7 after boost and was assessed for mFcγRIV activation against cells infected with 5 different clinical isolates (n = 5 mice/pool; data represented as mean, SD obtained from replicates). (**D**) Day 7 postboost serum from mice vaccinated with ΔgD-2, UVΔgD-2, HIΔgD-2, or VD60 lysates (control) were evaluated for anti-HSV antibodies by ELISA using an HSV-2–infected cell lysate (data represented as mean ±SD values of 5 mice/group) and (**E**) mFcγRIV activation against HSV-2(4674)–infected cells (lines represent means). Dashed lines represent values from mock-infected mouse serum. For **A** and **E**, $*P < 0.05$, $**P < 0.01$, $***P < 0.001$, ΔgD-2 vaccinated groups vs. control-vaccinated group via 2-way ANOVA. For **B**, **C**, and **D**, $*P < 0.05$, $**P < 0.01$, $***P < 0.001$; AUCs were generated for each group and then analyzed via one-way ANOVA comparing ΔgD-2, UVΔgD-2, or HIΔgD-2 groups with control values (**B** and **D**) or against each other (**C**).

live ΔgD-2 suggests that both structural (envelope glycoproteins such as gB (19), capsid, and/or tegument proteins) and infected cell proteins not packaged into virions likely contribute.

The notion that nonneutralizing, FcγR-activating Abs may be critical for HSV protection was suggested almost 20 years ago following the disappointing results of the gB-2/gD-2 subunit vaccine clinical trials (25, 26). The gB-2/gD-2 subunit vaccine induced high-titer gB- and gD-specific ELISA and HSV-2 neutralizing Abs, but in post-trial studies, there were low ADCC responses in the serum of vaccine participants (27). Similarly, the more recent clinically evaluated recombinant gD-2 protein vaccine elicited high-titer gD-specific and neutralizing Abs but was not protective. Whether the gD subunit vaccine elicited FcγR-activating Abs has not yet been reported. Together, these recombinant vaccine studies indicate that gD- and gB-neutralizing Abs are not sufficient for HSV-2 protection (9). In neonates, high ADCC Ab levels are associated with less severe neonatal disease (28), and in preliminary ongoing studies, we found that women with frequent symptomatic genital herpes outbreaks had higher neutralizing but lower FcγR-activating Abs compared with women with few or no clinical recurrences (data not shown). The findings from the ΔgD-2 vaccine coupled with clinical data support a role for FcγR effector functions in protection against both primary and recurrent disease.

The skin model also afforded the opportunity to more closely examine the local immune response to HSV. We observed a rapid inflammatory response characterized by increases in cytokines and chemokines in both control-vaccinated and ΔgD-2–vaccinated mice on day 2 after challenge. However, the

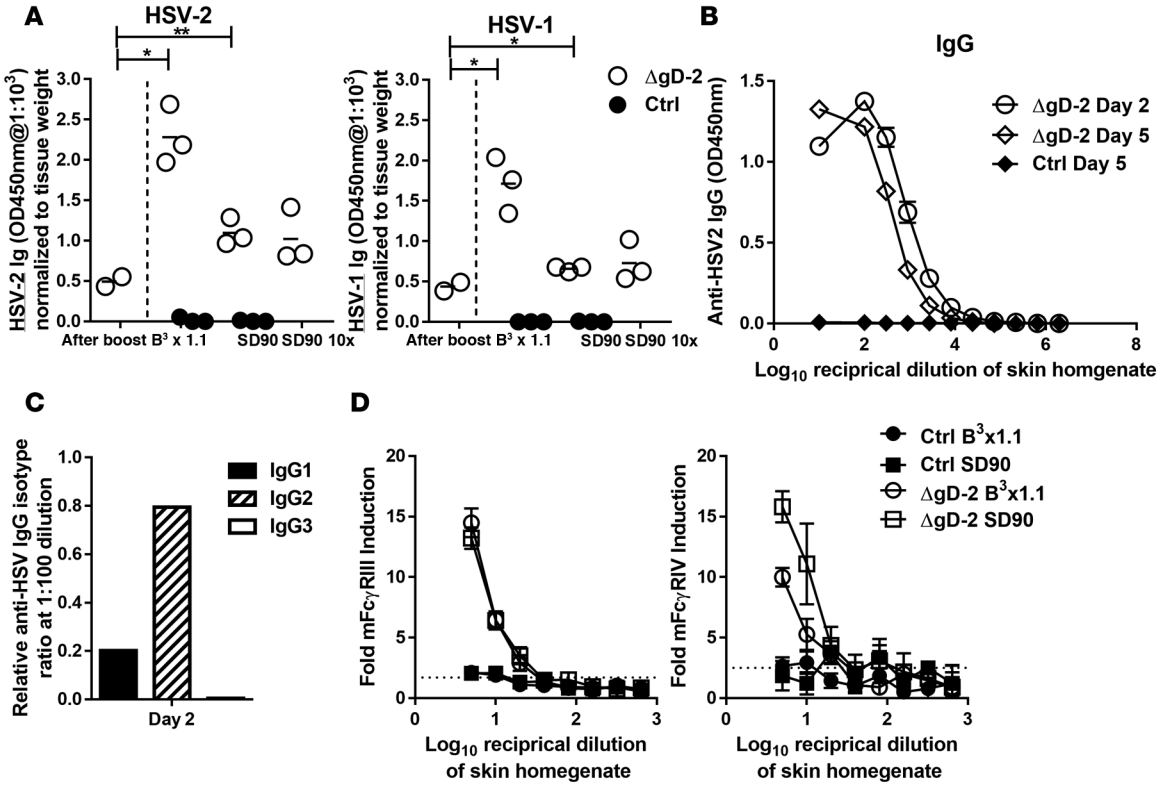

Figure 7. FcγR-activating HSV-specific IgG2 antibodies are rapidly recruited into the skin of ΔgD-2–vaccinated mice following viral challenge. Mice were immunized with ΔgD-2 or VD60 cell lysates (control) and subsequently challenged with HSV-1(B^3 × 1.1) and HSV-2(SD90) clinical isolates on the skin. (**A**) Skin biopsies were obtained 21 days after boost and day 2 after challenge, homogenized, and evaluated for the presence of anti-HSV antibodies by ELISA using an HSV-2–infected (left) or HSV-1–infected (right) cell lysate as the antigen (n = 3 mice per group, lines represent mean). Differences in HSV-specific Abs in ΔgD-2–vaccinated vs. control-vaccinated mice were compared by students t test; $^*P < 0.05$; $^{**}P < 0.01$. (**B**) Pools (6 mice per pool) of skin homogenates (at day 2 or day 5 after challenge) were serially diluted and assayed in an HSV-2 ELISA (results are mean ±SD obtained from testing pools in duplicate). (**C**) The relative proportion of different IgG subtypes in the day 2 postchallenge skin homogenate pool was determined using subtype-specific secondary antibodies in the ELISA. Results shown are with the 1:100 dilution of the pooled skin homogenates. (**D**) mFcγRIII (left panel) and mFcγRIV (right panel) activation was also assessed in pools of serially diluted skin homogenates (n = 3 mice/pool, mean ±SD obtained from testing pools in duplicate). Dashed lines represent mock-infected skin homogenate activation.

inflammatory response resolved in the vaccinated mice by day 5, which is consistent with the rapid clearance of virus, whereas inflammation persisted in the control-vaccinated mice, consistent with progressive disease. The latter was characterized by persistently elevated cytokines/chemokines (IL-1β, IL-6, CXCL9, and CXCL10) and neutrophils, which were observed throughout the epithelium and within the dermal layer in the control-vaccinated mice.

Interestingly, IL-33 was the only cytokine that trended higher in the skin from the ΔgD-2–immunized mice compared with controls. The precise role of IL-33 is not known. Prior studies have shown that recombinant IL-33 (rIL-33) administration enhanced skin wound healing in mice and was associated with activation of innate lymphoid cells and differentiation of monocytes into type 2 macrophages (29, 30). Systemic administration of IL-33 to mice was associated with an increase in FcγRIIb, which is linked to decreased inflammation (31). Possibly, the increase in IL-33 observed in the skin of ΔgD-2–vaccinated mice promoted wound healing and resolution of inflammation. Deciphering the role IL-33 plays in response to HSV warrants further study.

Consistent with other studies, we found that the clinical isolates displayed variable virulence in the murine skin (and vaginal) model despite similar in vitro growth kinetics (21, 32). Interestingly, although we observed a similar level of genetic diversity among HSV-1 isolates to that described in previous studies, we found substantially greater genetic diversity among the HSV-2 isolates collected in the Bronx community than those described in previous reports. The greater differences observed here may reflect the diverse geographic origins of the Bronx community. Despite this heterogeneity, all of the isolates tested were completely protected by ΔgD-2 vaccine and were able to activate the FcγR when cultured with target

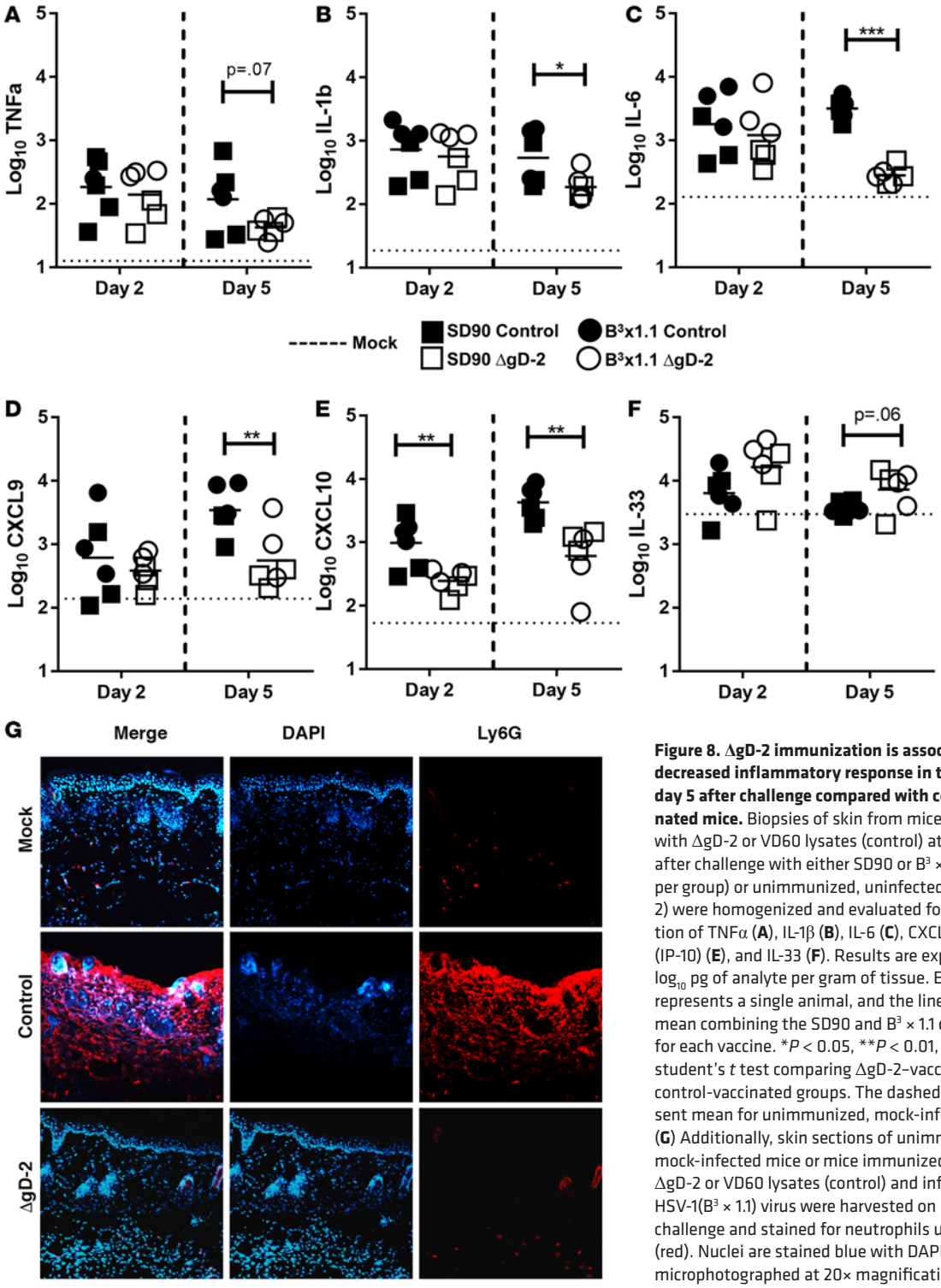

Figure 8. ΔgD-2 immunization is associated with decreased inflammatory response in the skin by day 5 after challenge compared with control-vaccinated mice. Biopsies of skin from mice immunized with ΔgD-2 or VD60 lysates (control) at day 2 or day 5 after challenge with either SD90 or $B^3 \times 1.1$ (n = 3 mice per group) or unimmunized, uninfected controls (n = 2) were homogenized and evaluated for concentration of TNFα (**A**), IL-1β (**B**), IL-6 (**C**), CXCL9 (**D**), CXCL10 (IP-10) (**E**), and IL-33 (**F**). Results are expressed as $\log_{10}$ pg of analyte per gram of tissue. Each dot represents a single animal, and the lines represent mean combining the SD90 and $B^3 \times 1.1$ challenges for each vaccine. $^*P < 0.05$, $^{**}P < 0.01$, $^{***}P < 0.001$, student's t test comparing ΔgD-2–vaccinated vs. control-vaccinated groups. The dashed lines represent mean for unimmunized, mock-infected animals. (**G**) Additionally, skin sections of unimmunized mock-infected mice or mice immunized with HSV-2 ΔgD-2 or VD60 lysates (control) and infected with HSV-1($B^3 \times 1.1$) virus were harvested on day 5 after challenge and stained for neutrophils using Ly6G (red). Nuclei are stained blue with DAPI. Images were microphotographed at 20× magnification.

cells infected with different clinical isolates, possibly reflecting a polyantigenic response. The complete protection against both HSV-1 and HSV-2 is clinically relevant, as HSV-1 has emerged as the more common cause of genital disease in the developed world (1).

The broad protection observed here in skin and vaginal models combined with the sterilizing immunity, as evidenced by absence of latent virus, support further development of the ΔgD-2 vaccine. To date, ΔgD-2 has protected 180 mice from lethal challenge (100%) and 94 of 95 mice from latency, as measured by qPCR for viral DNA or ex vivo reactivation. The findings also suggest that FcγR activation may provide

a better correlate of immune protection. Moreover, the ability of ΔgD-2 to elicit nonneutralizing FcγR antibodies provides an intriguing vaccine vector for generating protective vaccines against other pathogens such as HIV where nonneutralizing FcγR-functioning Abs have been shown to correlate with protection (33–35).

Methods

Cells and viruses. Vero (African green monkey kidney cell line; CCL-81; American Type Culture Collection [ATCC]) cells, VD60 cells (Vero cells encoding *gD-1* under endogenous promoter, ref. 36), and CaSki (human cervical epithelial cell line; CRL-1550; ATCC) were passaged in DMEM supplemented with 10% FBS (Gemini Bio-Products). THP-1 cells (human monocyte cell line; TIB-202; ATCC) were passaged in RPMI-1640 (Invitrogen) supplemented with 10% FBS. Laboratory strains HSV-2(G) (37), HSV-2 (333-ZAG) (38), HSV-1(17) (39), and HSV-1(F) (37) were propagated on Vero cells. Previously described clinical isolates HSV-2(4674) (38) and HSV-2(SD90) (South African isolate provided by David Knipe, Harvard Medical School, Boston, Massachusetts, USA) (17) were propagated on CaSki and Vero cells, respectively. Ten additional deidentified clinical isolates (five HSV-2 isolates designated $B^3 \times 2.1$ through $B^3 \times 2.5$ and five HSV-1 isolates designated $B^3 \times 1.1$ through $B^3 \times 1.5$) were provided by the Montefiore Clinical Virology Lab (Amy Fox, Montefiore Medical Center, Bronx, New York, USA) and passaged 3 times on Vero cells for a low-passage working stock. Construction of the single-cycle vaccine candidate strain, HSV-2(G) ΔgD-2, and its propagation on VD60 cells has been previously described (18, 19). Inactivation of virus was performed by exposing ΔgD-2 stocks to UV light for 10 minutes (10 cm distance from light source, ref. 23) or by heating to 60°C for 5 minutes. The impact of UV or HI on viral gene expression and infectivity was assessed by isolating RNA from Vero cells infected with 5 PFU/cell 2 and 6 hours after infection and performing reverse transcription PCR (RT-PCR) for infected cell protein-0 (ICP0) or thymidine kinase (TK) by using primers from Applied Biosystems (Carlsbad, California, USA) and conducting plaque assays on VD60 cells, respectively.

Murine immunization and viral challenge studies. Female C57BL/6 and BALB/c mice were purchased from the Jackson Laboratory (JAX) at 4–6 weeks of age. Mice were primed and boosted 3 weeks later with 5×10^4 to 5×10^6 PFU of ΔgD-2, 5×10^6 PFU UV-inactivated ΔgD-2, 5×10^6 PFU HI ΔgD-2, or an equal amount of uninfected VD60 cell lysates (control) s.c. (medial to the hind limb and pelvis) at 100 μl/mouse.

For intravaginal HSV infections, mice were treated with 2.5 mg of medoxyprogesterone acetate (MPA; Sicor Pharmaceuticals) s.c. 5 days prior to challenge. Mice were then inoculated intravaginally with an LD90 (5×10^5 PFU/mouse) of HSV-2(4674) at 30 μl/mouse and scored for disease and monitored for survival for 14 days as previously described (19).

For HSV skin infections, mice were depilated on the right flank with Nair and allowed to rest for 24 hours. Depilated mice were anesthetized with isoflurane (Isothesia, Henry-Schein); they were then abraded on the exposed skin with a disposable emory board for 20–25 strokes and subsequently challenged with 1×10^5 PFU HSV-1 or 5×10^4 PFU HSV-2 strains for in vivo virulence studies or challenged with an LD90, 10 times LD90, or 100 times LD90 of select HSV strains (see Table 1). Mice were monitored for 14 days and scored as follows: 1, primary lesion or erythema; 2, distant site zosteriform lesions, mild edema/erythema; 3, severe ulceration and edema, increased epidermal spread; 4, hind-limb paresis/paralysis; and 5, death. Mice that were euthanized at a score of 4 were assigned a value of 5 on all subsequent days for statistical analyses.

In vitro growth curves. For single-step growth of each virus, Vero cells were infected with virus at an MOI of 5 PFU/cell, and supernatants and cells were collected every 4, 8, 16, and 24 hours after infection and stored at −80°C. For multistep growth of each virus, Vero cells were infected at a MOI of 0.01 PFU/cell, and supernatants and cells were harvested every 12 hours after infection up to 72 hours. Infectious virus was measured by performing plaque assays with supernatants and lysed cells as previously described (38).

Viral DNA isolation and sequencing of clinical isolates. HSV DNA was prepared by infecting confluent Vero cells in a T150 flask with different clinical isolates or HSV-2(G) at an MOI of 10. Cells were harvested 16 hours after infection and washed twice with PBS. DNA was extracted using DNeasy Blood and Tissue (Qiagen) following the manufacturer's recommendations. DNA was quantitated by Qubit dsDNA HS assay (Invitrogen). Paired-end libraries were prepared by the Nextera XT DNA library preparation kit (Illumina) following the manufacturer's instructions. Libraries were sequenced on a Illumina MiSeq Desktop Sequencer. Viral genome sequences were assembled with the VirAmp pipeline (40) following removal of host sequence by alignment to the *Macaca mulatta* genome as a substitute for the incomplete *Chlorocebus*

sabaeus (source of Vero cells) genome. HSV-1 and HSV-2 genomes were annotated with Genome Annotation Transfer Utility on ViPR by comparison to HSV-1(17) (GenBank accession no. JN555585.1) and HSV-2(HG52) (JN561323) prior to submission to GenBank. Whole genome alignments including the previously sequenced HSV-2(SD90e) (KF781518), HSV-2(333) (KP192856), ChHV 105640 (NC_023677.1), and HSV-1(F) (GU734771.1) were performed using ClustalW (41), and phylogenetic trees were constructed using the unweighted pair group method with arithmetic mean (UPGMA) with 1,000 bootstrap replicates in Molecular Evolutionary Genetics Analysis v.6 (MEGA6) (42). All positions containing gaps or missing data were eliminated. GenBank numbers for newly sequenced genomes are as follows: HSV-2(G) (KU310668), HSV-2(4674) (KU310667), $B^3 \times 1.1$ (KU310657), $B^3 \times 1.2$ (KU310658), $B^3 \times 1.3$ (KU310659), $B^3 \times 1.4$ (KU310660), $B^3 \times 1.5$ (KU310661), $B^3 \times 2.1$ (KU310662), $B^3 \times 2.2$ (KU310663), $B^3 \times 2.3$ (KU310664), $B^3 \times 2.4$ (KU310665), and $B^3 \times 2.5$ (KU310666).

Virus detection in tissue. Skin biopsies (~5–10 mm in diameter by mechanical excision) and DRG were obtained from ΔgD-2 or VD60 lysates immunized mice at day 2, 5, 7, 14, or 21 after viral skin challenge. The tissue was weighed and homogenized in RNase/DNase free Lysing Matrix A tubes (MP Biomedicals) with serum-free DMEM at 6.0 m/sec for three 30-second cycles in the FastPrep-24 5G (MP Biomedicals). Samples were spun at 2,500 × *g* for 10 minutes at 4°C, and the resulting supernatant was overlaid on confluent Vero cell monolayers (2×10^5 cells/well in a 48-well plate) for 1 hour to measure replicating virus via plaque assay. Wells were washed with PBS and then with 199 medium (Gibco) containing 1% heat-inactivated FBS, overlaid with 0.5% methylcellulose and incubated at 37°C for 48 hours. Cells were fixed with 2% paraformaldehyde and stained with a crystal violet solution, and the number of PFU was quantified. Neuronal ex vivo coculture assays were performed at day 5 after challenge as previously described (19).

HSV qPCR. DNA was extracted from weighed tissue samples using DNeasy Blood and Tissue (Qiagen) following the manufacturer's recommendations. Extracted DNA was then normalized to 10 ng of DNA per reaction and viral DNA quantified using qPCR using ABsolute qPCR ROX Mix (Thermo Scientific). Primers for HSV polymerase (U_L30) were purchased from Integrated DNA Technologies (forward primer sequence 5′-GGCCAGGCGCTTGTTGGTGTA-3′, reverse primer sequence 5′-ATCACCGACCCGGAGAGGGA-3′, probe sequence 5′-CCGCCGAACTGAGCAGACACCCGC-3 ′) and used to detect viral genomic DNA. Isolated HSV-2 viral DNA was calibrated for absolute copy amounts using QuantStudio 3D Digital PCR (dPCR, ThermoFisher Scientific) and subsequently used as a standard curve to determine HSV viral genome copies. Samples that read 4 or fewer copy numbers were considered negative. Data are presented as $\log_{10}$ HSV genomes per gram of DRG tissue.

Histopathology and immunofluorescence of skin tissue. Mice were euthanized on day 5 after challenge, and the skin at the infection site was excised and either frozen in optimal cutting temperature (OCT) media, cut into 5-μm sections and stored at –80°C for immunofluorescence, or formalin fixed for 48 hours at room temperature (RT), paraffin-embedded, and sectioned for histopathology. Slides from paraffin-embedded sections were stained with H&E and evaluated by a board-certified veterinary pathologist who was blinded to the identity of the samples. The slides for immunofluorescent studies were fixed in –20°C acetone for 15 minutes, washed with wash buffer (0.05% Tween 20 in PBS), blocked for 2 hours with blocking buffer (2% BSA, 5% heat inactivated goat serum in PBS) at RT, and washed twice with wash buffer (WB). Slides were then incubated with anti-Ly6G (clone 1A8, 1:500, BD Biosciences) in blocking buffer for 1 hour at RT, washed, and incubated with a goat anti-rat secondary antibody conjugated with Alexa Flour 555 (1:500, ThermoFisher Scientific) for 30 minutes at RT. Slides were washed and mounted with media containing DAPI (ProLong Diamond Antifade Mountant with DAPI, ThermoFisher Scientific). Slides were imaged using a Nikon Eclipse Ti-U inverted light microscope at 20× magnification from apical layer (epidermal) to basal layer (striated muscle) at 2 different locations per sample.

Detection of antibodies and cytokines in skin biopsies and serum. Skin biopsies were obtained from HSV-2 ΔgD-2– or VD60 lysate–immunized (control-immunized) mice (~5–10 mm in diameter by mechanical excision) day 21 after boost or day 2 and 5 after viral skin challenge. The tissue was weighed and homogenized as described above and was evaluated for presence of anti-HSV antibodies, cytokines, and chemokines. Serum was also analyzed for HSV-2 antibodies from HSV-2 ΔgD-2– or control-immunized mice collected before immunization, 1 week after prime, or 1 week after boost. Anti-HSV antibodies were detected by ELISA as previously described using uninfected, HSV-1(17)–infected, or HSV-2(4674)–infected Vero cell lysates as the coating antigen (19). Biotin anti–mouse Igκ (clone 187.1) or biotin anti-mouse IgA (clone C10-1), IgM (clone I1/41), IgG1 (clone A85-1), IgG2a (clone R19-15), IgG2b (clone R12-3), or IgG3 (clone R40-82) at

1 μg/ml (all from BD Biosciences) were used as secondary detection antibodies. Wells were read on a SpectraMax (M5 series) ELISA plate reader at an absorbance of 450 nm. The resulting absorbance was determined by subtracting values obtained for uninfected cell lysates to values obtained with infected cell lysates. Total anti–HSV Ig is reported as the optical density (OD) at 450nm normalized to relative tissue weight at a 1:1,000 dilution of tissue homogenate. Anti–HSV IgG, IgA, IgM, or IgG1-3 are reported as the OD at 450 nm at all dilutions except IgG1-3, which is reported only at a 1:100 dilution of skin homogenate.

Skin homogenate supernatants were assayed for IL-6, IL-1β, IL-33, TNFα, monokine induced by IFN-γ (MIG, CXCL9), and IFN-inducible cytokine (IP-10, CXCL10) using a Milliplex mouse cytokine/chemokine immunoassay (Millipore) and a Luminex Magpix system and analyzed with Milliplex Analyst (Version 3.5.5.0; VigeneTech Inc.).

ADCP assay. To determine HSV-specific ADCP, a protocol modified from Ackerman, et al. (43), was used. Briefly, 2×10^8 1 μm Neutravadin-red fluorescent beads (Invitrogen, F-8775) were coated with 0.3 mg of biotinylated HSV-2–infected or uninfected (control) Vero cells overnight at 4°C in 500 μl of Block-Aid (ThermoFisher Scientific, B-10710). Beads were washed twice with 1% BSA in PBS, and then 1×10^6 beads/well were added to a 96-well round-bottom plate. Of a 1:5 dilution (diluted in serum-free RPMI), 50 μl of 1-week postboost immune serum that had been heat-inactivated at 56°C for 30 minutes were added to the wells and incubated for 2 hours at 37°C. THP-1 cells (2×10^4 cells/well) were then added to each well at a final volume of 200 μl/well and incubated for 8 hours at 37°C at 5% CO_2. Subsequently, 100 μl of supernatant was removed and stored at –20°C and then resuspended with 100 μl 4% paraformaldehyde. Samples were read on 5-laser LSRII flow cytometer (BD Biosciences) at the Einstein Flow Cytometry Core Facility. Phagocytic score is reported by gating on events representing THP-1 cells then applying the following equation: [(% of cells bead positive × MFI of cells positive for beads)/10^6] using FlowJo software (version 10, Tree Star Inc.). IFN-γ secretion from activated THP-1 cells via antibody phagocytosis was determined in parallel by analyzing stored cultured supernatants using a Milliplex human custom immunoassay (Millipore) and a Luminex Magpix system as previously described.

FcγR activation reporter assay. To determine HSV-specific FcγR activation of Abs, we utilized Promega's Fc effector murine and bioassay kits (a gift from Mei Cong, Promega Corporation, Madison, Wisconsin, USA). The Ab samples included serial dilutions of mouse serum or skin homogenate obtained 1 week after boost or 2–7 days after skin challenge diluted in serum-free RPMI. The Ab samples (25 μl) were incubated with target cells (1.25×10^4cells/well) in a 96-well plate for 30 minutes. The targets were Vero cells that had been infected for 16 hours with different strains of HSV-1 or HSV-2 (MOI 1 PFU/cell) or uninfected control cells. Jurkat cells stably expressing either murine FCγRIII ADCC reporter bioassay (mFcγRIII), mFcγRIV, and a downstream luciferase reporter gene based on NFAT activation acted as the effector source at a 6:1 effector/target ratio. The effector and target cells were incubated for 6 hours at 37°C, and luminescence was detected after the addition of 75 μl of Bio-Glo Reagent (Promega) and read on an SpectraMax M5 plate reader. Fold FcγR induction was calculated as luminescence of [(Ab sample with effector and target cells – luminescence of background)/(luminescence of spontaneous activation of effector cells by target cells alone – luminescence of background)].

Statistics. Results were compared by 2-way ANOVA with multiple comparisons or 2-tailed unpaired Student's *t* tests using GraphPad Prism version 6. Mantel-Cox survival curves were compared by log rank tests. *P* values < 0.05 (*), < 0.01 (**), < 0.001 (***) were considered significant.

Study approval. Murine animal experiments were performed with approval from Albert Einstein College of Medicine Institutional Animal Care and Use Committee, Protocol 20130913 and 20150805.

Author Contributions

CDP, WRJJ, and BCH designed the experiments and wrote the manuscript. CDP, BW, NK, CB, and RS conducted the experiments. CDP and BW acquired data and analyzed data.

Acknowledgments

We are grateful to Amy Fox for providing the HSV-1 and HSV-2 clinical isolates obtained from the Clinical Virology Lab at Montefiore. We also acknowledge the comparative pathology and histopathology core at Albert Einstein College of Medicine for their assistance and Mei Cong, Promega Corporation, for providing mFcγRIII and mFcγRIV activation kits. The authors declare no financial conflict of interest. This work is supported by NIH grants R01AI117321 (WRJJ and BCH), AI098925 (WRJJ), R01AI026170 (WRJJ) and R01AI065309 (BCH).

Address correspondence to: Betsy C. Herold, Professor of Pediatrics and Microbiology and Immunology, Albert Einstein College of Medicine. 1301 Morris Park Avenue, Bronx, NY 10461. Phone: 718.839.7460; E-mail: betsy.herold@einstein.yu.edu. Or to: William R. Jacobs Jr., Howard Hughes Medical Institute Investigator, Professor of Microbiology and Immunology, Albert Einstein College of Medicine. Phone: 718.678.1075; E-mail: jacobsw@hhmi.org.

1. Bernstein DI, et al. Epidemiology, clinical presentation, and antibody response to primary infection with herpes simplex virus type 1 and type 2 in young women. *Clin Infect Dis*. 2013;56(3):344–351.
2. Gnann JW, et al. Herpes Simplex Encephalitis: Lack of Clinical Benefit of Long-term Valacyclovir Therapy. *Clin Infect Dis*. 2015;61(5):683–691.
3. Looker KJ, et al. Global estimates of prevalent and incident herpes simplex virus type 2 infections in 2012. *PLoS One*. 2015;10(1):e114989.
4. Schaftenaar E et al. High seroprevalence of human herpesviruses in HIV-infected individuals attending primary healthcare facilities in rural South Africa. *PLoS ONE*. 2014;9(6):e99243.
5. Whitley RJ. Herpes simplex viruses. *Clin Infect Dis.* 1998;26(3):541–553.
6. Gray RH, et al. Probability of HIV-1 transmission per coital act in monogamous, heterosexual, HIV-1-discordant couples in Rakai, Uganda. *Lancet*. 2001;357(9263):1149–1153.
7. Schacker T, Zeh J, Hu HL, Hill E, Corey L. Frequency of symptomatic and asymptomatic herpes simplex virus type 2 reactivations among human immunodeficiency virus-infected men. *J Infect Dis*. 1998;178(6):1616–1622.
8. Todd J, et al. Effect of genital herpes on cervicovaginal HIV shedding in women co-infected with HIV AND HSV-2 in Tanzania. *PLoS One*. 2013;8(3):e59037.
9. Belshe RB et al. Correlate of immune protection against HSV-1 genital disease in vaccinated women. *J Infect Dis*. 2014;209(6):828–836.
10. Bourne N, et al. Herpes simplex virus (HSV) type 2 glycoprotein D subunit vaccines and protection against genital HSV-1 or HSV-2 disease in guinea pigs. *J Infect Dis*. 2003;187(4):542–549.
11. Bourne N, Milligan G, Stanberry L, Stegall R, Pyles R. Impact of immunization with glycoprotein D2/AS04 on herpes simplex virus type 2 shedding into the genital tract in guinea pigs that become infected. *J Infect Dis*. 2005;192(12):2117–2123.
12. Keadle TL, et al. Efficacy of a recombinant glycoprotein D subunit vaccine on the development of primary and recurrent ocular infection with herpes simplex virus type 1 in mice. *J Infect Dis*. 1997;176(2):331–338.
13. Newman RM, et al. Genome Sequencing and Analysis of Geographically Diverse Clinical Isolates of Herpes Simplex Virus 2. *J Virol*. 2015;89(16):8219–8232.
14. Szpara ML, et al. Genome Sequence of the Anterograde-Spread-Defective Herpes Simplex Virus 1 Strain MacIntyre. *Genome Announc*. 2014;2(6):6.
15. Kolb AW, Larsen IV, Cuellar JA, Brandt CR. Genomic, phylogenetic, and recombinational characterization of herpes simplex virus 2 strains. *J Virol*. 2015;89(12):6427–6434.
16. Lamers SL et al. Global Diversity within and between Human Herpesvirus 1 and 2 Glycoproteins. *J Virol*. 2015;89(16):8206–8218.
17. Dudek TE, Torres-Lopez E, Crumpacker C, Knipe DM. Evidence for differences in immunologic and pathogenesis properties of herpes simplex virus 2 strains from the United States and South Africa. *J Infect Dis*. 2011;203(10):1434–1441.
18. Cheshenko N, et al. HSV activates Akt to trigger calcium release and promote viral entry: novel candidate target for treatment and suppression. *FASEB J*. 2013;27(7):2584–2599.
19. Petro C, et al. Herpes simplex type 2 virus deleted in glycoprotein D protects against vaginal, skin and neural disease. *Elife*. 2015;4.
20. Schiffer JT, Corey L. Rapid host immune response and viral dynamics in herpes simplex virus-2 infection. *Nat Med*. 2013;19(3):280–290.
21. Sydiskis RJ, Schultz I. Herpes Simplex Skin Infection in Mice. *J Infect Dis*. 1965;115:237–246.
22. Nixon B, et al. Griffithsin protects mice from genital herpes by preventing cell-to-cell spread. *J Virol*. 2013;87(11):6257–6269.
23. Fakioglu E, et al. Herpes simplex virus downregulates secretory leukocyte protease inhibitor: a novel immune evasion mechanism. *J Virol*. 2008;82(19):9337–9344.
24. Nimmerjahn F, Bruhns P, Horiuchi K, Ravetch JV. FcgammaRIV: a novel FcR with distinct IgG subclass specificity. *Immunity*. 2005;23(1):41–51.
25. Langenberg AG, et al. A recombinant glycoprotein vaccine for herpes simplex virus type 2: safety and immunogenicity [corrected]. *Ann Intern Med*. 1995;122(12):889–898.
26. Corey L, et al. Recombinant glycoprotein vaccine for the prevention of genital HSV-2 infection: two randomized controlled trials. Chiron HSV Vaccine Study Group. *JAMA*. 1999;282(4):331–340.
27. Kohl S, et al. Limited antibody-dependent cellular cytotoxicity antibody response induced by a herpes simplex virus type 2 subunit vaccine. *J Infect Dis*. 2000;181(1):335–339.
28. Kohl S. Role of antibody-dependent cellular cytotoxicity in neonatal infection with herpes simplex virus. *Rev Infect Dis*. 1991;13 Suppl 11:S950–S952.
29. Yin H, et al. IL-33 accelerates cutaneous wound healing involved in upregulation of alternatively activated macrophages. *Mol Immunol*. 2013;56(4):347–353.
30. Rak GD, et al. IL-33-Dependent Group 2 Innate Lymphoid Cells Promote Cutaneous Wound Healing. *J Invest Dermatol*. 2016;136(2):487–496.
31. Anthony RM, Kobayashi T, Wermeling F, Ravetch JV. Intravenous gammaglobulin suppresses inflammation through a novel T(H)2 pathway. *Nature*. 2011;475(7354):110–113.
32. Simmons A, Nash AA. Zosteriform spread of herpes simplex virus as a model of recrudescence and its use to investigate the

role of immune cells in prevention of recurrent disease. *J Virol*. 1984;52(3):816–821.
33. Corey L, et al. Immune correlates of vaccine protection against HIV-1 acquisition. *Sci Transl Med*. 2015;7(310):310rv7.
34. Ackerman ME, et al. Polyfunctional HIV-Specific Antibody Responses Are Associated with Spontaneous HIV Control. *PLoS Pathog*. 2016;12(1):e1005315.
35. Chung AW, et al. Polyfunctional Fc-effector profiles mediated by IgG subclass selection distinguish RV144 and VAX003 vaccines. *Sci Transl Med*. 2014;6(228):228ra38.
36. Ligas MW, Johnson DC. A herpes simplex virus mutant in which glycoprotein D sequences are replaced by beta-galactosidase sequences binds to but is unable to penetrate into cells. *J Virol*. 1988;62(5):1486–1494.
37. Ejercito PM, Kieff ED, Roizman B. Characterization of herpes simplex virus strains differing in their effects on social behaviour of infected cells. *J Gen Virol*. 1968;2(3):357–364.
38. Nixon B, et al. Griffithsin protects mice from genital herpes by preventing cell-to-cell spread. *J Virol*. 2013;87(11):6257–6269.
39. Brown SM, Ritchie DA, Subak-Sharpe JH. Genetic studies with herpes simplex virus type 1. The isolation of temperature-sensitive mutants, their arrangement into complementation groups and recombination analysis leading to a linkage map. *J Gen Virol*. 1973;18(3):329–346.
40. Wan Y, Renner DW, Albert I, Szpara ML. VirAmp: a galaxy-based viral genome assembly pipeline. *Gigascience*. 2015;4:19.
41. Larkin MA, et al. Clustal W and Clustal X version 2.0. *Bioinformatics*. 2007;23(21):2947–2948.
42. Tamura K, Stecher G, Peterson D, Filipski A, Kumar S. MEGA6: Molecular Evolutionary Genetics Analysis version 6.0. *Mol Biol Evol*. 2013;30(12):2725–2729.
43. Ackerman ME, et al. A robust, high-throughput assay to determine the phagocytic activity of clinical antibody samples. *J Immunol Methods*. 2011;366(1-2):8–19.